

Semiclassical calculation of Coulomb break-up of weakly-bound nuclei

C.A. Bertulani¹

*National Superconducting Cyclotron Laboratory Michigan State University, East Lansing, MI
48824-1312, USA*

L.F. Canto

Instituto de Física, Universidade Federal do Rio de Janeiro, 21945, Rio de Janeiro, RJ, Brazil

Received 28 October 1991

Abstract: We develop a semiclassical coupled-channels calculation for the Coulomb break-up of loosely bound nuclei. The continuum wavefunctions are discretized by means of two different sets of strongly peaked functions: (a) a histogram set, and (b) a continuously derivable one. Using simple expressions for the bound and continuum wavefunctions, we calculate the break-up probability to first-order and with the coupled-channels method. First-order perturbation theory is shown to fail to describe the Coulomb break-up of unstable projectiles, as ^{11}Li at small impact parameters. It is shown that a non-perturbative calculation may reduce the cross section by 20% in collisions at intermediate energies.

1. Introduction

Coulomb excitation of unstable nuclei is a very useful technique to access information on the structure and excitation response function of such nuclei. This is especially true for the study of neutron- or proton-rich nuclei with very small binding energies. Such studies have been performed experimentally during the last years, resulting in the finding of new and intriguing aspects on their properties^{1,2}).

Many of the exotic nuclei, like ^{11}Li do not have a bound state besides the ground state, i.e., any excitation leads to their fragmentation. The Coulomb fragmentation cross section is roughly inversely proportional to the separation energy of the fragments³). Therefore, it can be very large for weakly bound projectiles incident on large- Z targets. Indeed, experimental studies on the break-up of weakly bound nuclei have shown that the contribution of the Coulomb interaction between the nuclei results in cross sections of several barns at bombarding energies of some tens of MeV per nucleon, and higher^{1,2}). That is an order of magnitude larger than the nuclear contribution to the process³).

One should expect that perturbation theory fails in describing the break-up process when the cross sections attain very high values. In fact, as we show in sect. 2 of this

¹ On leave of absence from: Instituto de Física, Universidade Federal do Rio de Janeiro, 21945 Rio de Janeiro, Brazil.

article, the break-up probability calculated with first-order perturbation theory is close to unity. This can be understood with use of simple arguments. The energy transferred by the Coulomb field to the excitation of a projectile nucleus, with N neutrons and Z protons, incident with velocity v on a target nucleus with charge eZ_T at an impact parameter b is approximately given by³⁾ $E^* = 2(NZ/A)(Z_T e^2)^2/m_N b^2 v^2$, where m_N is the nucleon mass. For ^{11}Li projectiles ($N = 8$, $Z = 3$) incident on lead at $b = 15$ fm and $v \approx c$, one gets $E^* \approx 0.3$ MeV. This energy is more than sufficient to break ^{11}Li apart, since the separation energy of two neutrons from this nucleus is about¹⁾ 0.25 MeV. This means that, at small impact parameters the break-up probability is of order of unity and a non-perturbative treatment of the break-up process should be carried out.

Non-perturbative techniques like semiclassical coupled-channels calculations can be used in this case. However, there are not many experimental data which justify a complicated calculation, with many details about the structure of the unstable nuclei. Since this is the final information that one wants to obtain, a clearer understanding of the reaction mechanism is more useful at this stage. The cluster model³⁾ seems to be very appropriate to achieve this goal. It has been used with success for the determination of the main characteristics of reactions induced by ^{11}Li projectiles³⁾ Owing to its simplicity the matrix elements of Coulomb break-up can be easily calculated.

This article is organized as follows: In sect. 2 we present a calculation of the Coulomb break-up of loosely bound clusters based on first-order time-dependent perturbation theory. We show that it fails to describe the Coulomb break-up probability at small impact parameters. In sect. 3 we present a coupled-channels calculation of Coulomb break-up, using discrete states built on continuum wavefunctions. The discretization procedure deserves special attention and we use two different sets of basis functions; a smooth and a step-wise one. In sect. 4 we compare the results of a numerical calculation of the coupled-channels equations with the first-order results. Our conclusions are given in sect. 5.

2. Coulomb break-up of loosely bound clusters

Let us consider a projectile nucleus composed of two clusters with charges eZ_b and eZ_c , and masses m_b and m_c , respectively, incident on a target with charge eZ_T . We assume that the projectile follows a straight-line trajectory with velocity v and impact parameter b . The interaction potential (neglecting magnetic interactions and nuclear forces) responsible for the break-up of the projectile, is given by

$$V = \gamma Z_T e^2 \left[\sum_{k=b,c} \frac{Z_k}{[(y_k - b)^2 + \gamma^2 (z_k - vt)^2]^{1/2}} - \sum_{k=b,c} \frac{Z_k}{(b^2 + \gamma^2 v^2 t^2)^{1/2}} \right], \quad (2.1)$$

where $\gamma = (1 - v^2/c^2)^{-1/2}$, and y_k , z_k represent the transverse and longitudinal coordinates of the particles, respectively.

In the dipole approximation, the expression (2.1) becomes

$$\begin{aligned}
 V &= \frac{\gamma Z_{\Gamma} e^2}{(b^2 + \gamma^2 v^2 t^2)^{3/2}} \sum_{k=b,c} Z_k (by_k + \gamma vt z_k) \\
 &= \sqrt{\frac{2\pi}{3}} \frac{\gamma Z_{\Gamma} e^2}{(b^2 + \gamma^2 v^2 t^2)^{3/2}} \left(Z_b \frac{m_c}{m_a} - Z_c \frac{m_b}{m_a} \right) \\
 &\quad \times r \left\{ ib \left[Y_{11}(\hat{\mathbf{r}}) + Y_{1-1}(\hat{\mathbf{r}}) \right] + \sqrt{2} \gamma vt Y_{10}(\hat{\mathbf{r}}) \right\}, \quad (2.2)
 \end{aligned}$$

where \mathbf{r} is the vector from b to c and $m_a = m_b + m_c$. The first (second) term inside the curly brackets represents the transverse (longitudinal) part of the interaction.

In first-order time-dependent perturbation theory, the probability amplitude for the projectile break-up, i.e., the transition from the ground state $|0\rangle$ to a state $|q\rangle$ in the continuum is given by

$$a_{(q)}^{(1)} = \frac{1}{i\hbar} \int_{-\infty}^t e^{-iE_0 - E_q)t'/\hbar} \langle q|V(t')|0\rangle dt'. \quad (2.3)$$

For loosely bound projectiles the ground state can be represented by an Yukawa wavefunction $\phi_0(\mathbf{r}) = Ne^{-\eta r}/r$, where N is the normalization factor, and $\eta = \sqrt{2\mu_{bc}B}/\hbar$, with μ_{bc} equal to the reduced mass of the $(b+c)$ system and B the binding energy. Neglecting final-state interactions, the states $|q\rangle$ are given by $\phi_q(\mathbf{r}) = \langle \mathbf{r}|q\rangle = e^{iq \cdot \mathbf{r}} + e^{iqr}/r(\eta + iq)$, where the wavenumber q is related to the energy E_q as $E_q = \hbar^2 q^2/2\mu_{bc}$. The second term of $\langle \mathbf{r}|q\rangle$ guarantees the orthogonality and completeness of the initial and final states.

The dipole matrix elements are given by³⁾

$$\langle q|rY_{1m}(\hat{\mathbf{r}})|0\rangle = i4\sqrt{2\pi\eta} \frac{q}{(q^2 + \eta^2)^2} Y_{1m}(q). \quad (2.4)$$

To first order, the break-up probability is obtained by integrating the square modulus of (2.3) over the density of final states, i.e.,

$$P^{(1)}(b, t) = 2P_{m=1}^{(1)} + P_{m=0}^{(1)} = \int |a_{(q)}^{(1)}|^2 \frac{d^3q}{(2\pi)^3}, \quad (2.5)$$

summed over the beam-axis components of the angular momentum carried by the Coulomb field, $m = 0, \pm 1$. The integral over q is easily accomplished if one uses the sudden approximation, which is valid for

$$\frac{b}{\gamma v} (E_q + B) \ll 1. \quad (2.6)$$

For weakly bound nuclei, as ^{11}Li , $E_q + B \approx 1$ MeV, and at bombarding energies $E_{\text{lab}} \sim 1$ GeV, the above relation shows that the sudden approximation is valid for impact parameters $b < 300$ fm.

Within the sudden approximation we can omit the exponential factor in (2.3) and the integrals can be evaluated analytically as (α is the fine-structure constant)

$$P^{(1)}(b, t) = \frac{1}{6} \left(\frac{Z_T \alpha c}{\eta b v} \right)^2 \left(Z_b \frac{m_c}{m_a} - Z_c \frac{m_b}{m_a} \right)^2 \times \left\{ \left[1 + \frac{\gamma v t / b}{\sqrt{1 + (\gamma v t / b)^2}} \right]^2 + \frac{1}{1 + (\gamma v t / b)^2} \right\}. \quad (2.7)$$

The first (second) term inside the curly brackets arises from the transverse (longitudinal) part of the interaction potential (2.2). It is clear that only the transverse contribution survives at $t = \infty$. The longitudinal contribution cancels since the component of the electric field along the beam axis is an odd function of time. The break-up probability at $t = \infty$ is given by

$$P^{(1)}(b, \infty) = \frac{2}{3} \left(\frac{Z_T \alpha c}{\eta b v} \right)^2 \left(Z_b \frac{m_c}{m_a} - Z_c \frac{m_b}{m_a} \right)^2. \quad (2.8)$$

For grazing collisions with heavy targets at high energies the break-up probabilities of eq. (2.8) are close to (or even exceeds) unity. Therefore, first-order perturbation theory cannot be used. However, if the sudden approximation holds a non-perturbative closed expression can still be derived. The amplitude can then be written as [neglecting the longitudinal component of the interaction potential (2.2)]

$$a_{(q)}^{(S)} = \langle q | \exp \left\{ \frac{1}{i\hbar} \int_{-\infty}^{\infty} V(t) dt \right\} | 0 \rangle = \langle q | \exp \{ -iCr \sin \theta \sin \phi \} | 0 \rangle, \quad (2.9)$$

where

$$C = \frac{2Z_T \alpha c}{bv} \left(Z_b \frac{m_c}{m_a} - Z_c \frac{m_b}{m_a} \right). \quad (2.10)$$

Using the completeness relation

$$\phi_0(\mathbf{r}) \phi_0^*(\mathbf{r}') + \frac{1}{(2\pi)^3} \int \phi_q^*(\mathbf{r}) \phi_q(\mathbf{r}') d^3q = \delta(\mathbf{r} - \mathbf{r}'), \quad (2.11)$$

one finds

$$P^{(S)}(b) = \int |a_{(q)}^{(S)}|^2 \frac{d^3q}{(2\pi)^3} = 1 - \frac{\eta^2}{4\pi^2} \left| \int d^3r \frac{e^{-2\eta r}}{r^2} e^{-iCr \sin \theta \sin \phi} \right|^2. \quad (2.12)$$

The above integral can be easily evaluated and the result is

$$P^{(S)}(b) = 1 - \frac{4\eta^2}{C^2} \left[\arctan \left(\frac{C}{2\eta} \right) \right]^2. \quad (2.13)$$

When $\frac{1}{2}C\eta \ll 1$ (large impact parameters) the above relation reproduces the first-order result (2.8). If, on the other hand, C/η is large, one gets to lowest order in η/C ,

$$P^{(S)}(b) = 1 - \frac{\pi^2 \eta^2}{C^2}. \quad (2.14)$$

A comparison between the sudden approximation and the first order break-up probabilities for the reaction $^{11}\text{Li} + \text{Pb} \rightarrow ^9\text{Li} + 2n + \text{Pb}$ at 100 MeV/nucleon, is shown in fig. 1 as a function of b . The failure of the first-order approximation (dashed line) at small impact parameters is clearly seen.

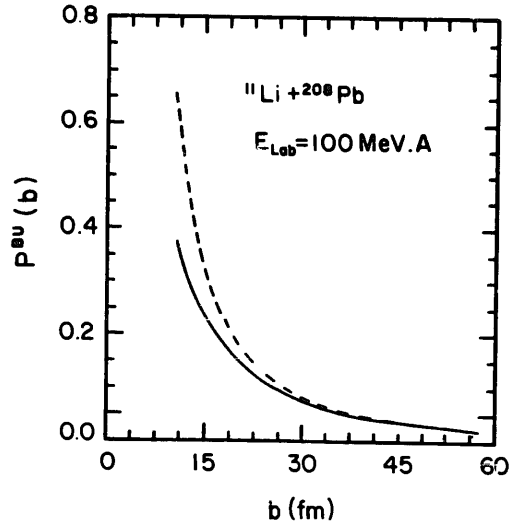


Fig. 1. Coulomb break-up probabilities of ^{11}Li projectiles incident on lead at 100 MeV/nucleon, as a function of the impact parameter b .

The results of eqs. (2.7), (2.8) and (2.13) were obtained on the basis of the sudden approximation. In the example considered, the ^{11}Li break-up probability is appreciable even for large relative energies in the projectile frame ($E_q \sim 2$ MeV), where the sudden approximation starts to break-down. In addition, the treatment of this section cannot account for the energy distribution of the break-up cross section. A more powerful coupled-channels treatment is therefore desirable. However, one faces the difficulty that the final states are in the continuum (one would have to consider a continuous channel label) and the coupling matrix elements present divergency problems, caused by the non-localized behavior of the continuum wavefunctions. This difficulty is avoided by a discretization of the continuum along the lines proposed by Bär and Soff⁴) in their non-perturbative calculations of atomic ionization by heavy ions. In the next section we use a similar treatment of the continuum and develop a set of semiclassical coupled-channels equations.

3. Discretization of the continuum and semiclassical treatment of the coupled-channels problem

Our basis of time-dependent discrete states are defined as

$$\begin{aligned}
 |\phi_0\rangle &= e^{-iE_0 t/\hbar} |0\rangle, \quad \text{with} \quad E_0 = -B, \\
 |\phi_{jlm}\rangle &= e^{-iE_j t/\hbar} \int \Gamma_j(E) |E, lm\rangle dE,
 \end{aligned} \tag{3.1}$$

where $|E, lm\rangle$ are continuum wavefunctions of the projectile fragments (without the interaction with the target), with good energy and angular momentum quantum numbers E, l, m . The functions $\Gamma_j(E)$ are assumed to be strongly peaked around an energy E_j in the continuum. Therefore, the discrete character of the states $|\phi_{jlm}\rangle$ (together with

$|\phi_0\rangle$) allows an easy implementation of the coupled-states calculations. We assume that the projectile has no bound excited states. This assumption is often the rule for very loosely bound systems. The orthogonality of the discrete states (3.1) is guaranteed if

$$\int dE \Gamma_i(E) \Gamma_j(E) = \delta_{ij}, \quad (3.2)$$

For the continuum set $|Elm\rangle$ we use, for the sake of simplicity, the plane-wave basis

$$\langle r|Elm\rangle = u_{l,E}(r) Y_{lm}(\mathbf{r}) = \left(\frac{2\mu}{\hbar^2}\right)^{3/4} \frac{E^{1/4}}{\sqrt{\pi}} j_l(qr) Y_{lm}(\hat{\mathbf{r}}), \quad (3.3)$$

which obey the normalization condition ($E = \hbar^2 q^2 / 2\mu$)

$$\langle Elm|E'l'm'\rangle = \delta_{ll'} \delta_{mm'} \delta(E - E'). \quad (3.4)$$

These states arise from the partial wave expansion of the plane wave $\exp(i\mathbf{q}\cdot\mathbf{r})$. Writing the time-dependent Schrödinger equation for $\Psi(t) = \sum_j a_{jlm} \phi_{jlm}$, taking the scalar product with the basis states and using orthonormality relations, we get the equations

$$i\hbar \frac{da_{jlm}}{dt} = \sum_{j'l'm'} V_{jlm;j'l'm'} a_{j'l'm'} e^{-i(E'_j - E_j)t/\hbar}. \quad (3.5)$$

We use the index $j = 0$ for the ground state $|0\rangle$ and $j = 1, 2, \dots$ for the discrete continuum states. $V_{jlm;j'l'm'}$ are the matrix elements $\langle \phi_{jlm} | V | \phi_{j'l'm'} \rangle$.

For $\Gamma_j(E)$ we consider two different sets of functions. Firstly the set $\Gamma_1(E), \dots, \Gamma_N(E)$:

$$\begin{aligned} \Gamma_j(E) &= \frac{1}{\sqrt{\sigma}}, & \text{for } (j-1)\sigma < E < j\sigma \\ &= 0, & \text{otherwise.} \end{aligned} \quad (3.6)$$

This set corresponds to histograms of constant height $1/\sqrt{\sigma}$ and width σ . The states $\Gamma_j(E)$ trivially satisfy the orthonormalization condition of eq. (3.2). They present the advantage of leading to simple analytical expressions for the coupling matrix elements. On the other hand they have discontinuities at the edges, which lead to numerical difficulties. The second set consists of the functions

$$\chi_j(E) = N_{n_j} \left(\frac{E}{\sigma}\right)^{n_j} e^{-n_j(E/\sigma)}. \quad (3.7a)$$

The normalization constant

$$N_{n_j} = \frac{1}{\sqrt{\sigma}} \left[\frac{(2n_j)^{2n_j+1}}{(2n_j)!} \right]^{1/2}, \quad (3.7b)$$

guarantees that $\int \chi_j(E) \chi_j(E) dE = 1$. The functions χ_j are peaked at $E = n_j \sigma$ and have width $\approx \sigma$. The integer $n_j = Kj$ is proportional to the index- j and the proportionality constant, a small integer K , is a parameter of the set which determines the overlap of two consecutive functions χ_j and χ_{j+1} . Three consecutive functions χ_4, χ_5 and χ_6 are shown in fig. 2a for $K = 3$ and $\sigma = \frac{40}{3}$ keV. With this choice χ_5 is

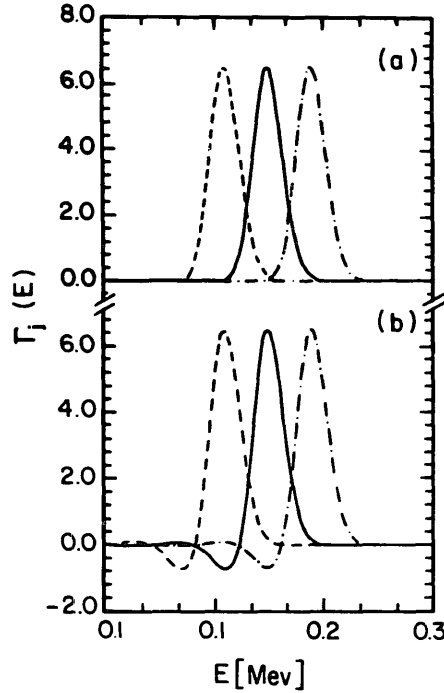


Fig. 2. A set of functions given by the expression (3.7a) of text, before (a) and after (b) orthogonalization.

peaked at the maximum of the experimental break-up cross section ($E \approx 200$ keV) of ^{11}Li projectiles (see fig. 5). However, this set fails to satisfy the orthogonality condition of eq. (3.2). This shortcoming can be fixed by the definition of a new set $\Gamma_j(E)$ of linear combinations

$$\Gamma_j(E) = \sum_{k=1}^N C_{jk} \chi_k(E), \quad (3.8)$$

with the coefficients C_{ij} determined so that the resulting combinations be orthogonal. These coefficients can be found by means of an orthogonalization procedure as, e.g., the Gram-Schmidt method⁵). The result of the application of this method to the functions of fig. 2a is shown in fig. 2b. The set of eq. (3.8) has the advantages of being continuously derivable and of leading to reasonably simple coupling matrix elements.

A comparison between basis states $\phi_{jlm}(r)$ generated with each of these sets [through eq. (3.1)] is made in figs. 3a and 3b. We chose for convenience the parameters $\sigma = 40$ keV, $j = 5$ for the first set (eq. (3.6)) and $K = 3$, $j = 5$, $\sigma = 13.3$ keV for the second set (eq. (3.7)). With this choice one of the E_j is equal to 200 keV for both sets. We take $l = 1$, $m = 1$, as example. One observes that the discrete wavefunctions ϕ_{jlm} decrease rapidly enough with r , so that the matrix elements $\langle \phi_{j'l'm'} | r Y_{1\mu} | \phi_{jlm} \rangle$ are finite. The use of the histograms (3.6) for $\Gamma_j(E)$ leads to beats in ϕ_{jlm} as displayed in fig. 3a. These beats are the result of the discontinuous nature of $\Gamma_j(E)$ and arise from the interference from the borders of the histograms. Due to this behaviour, the

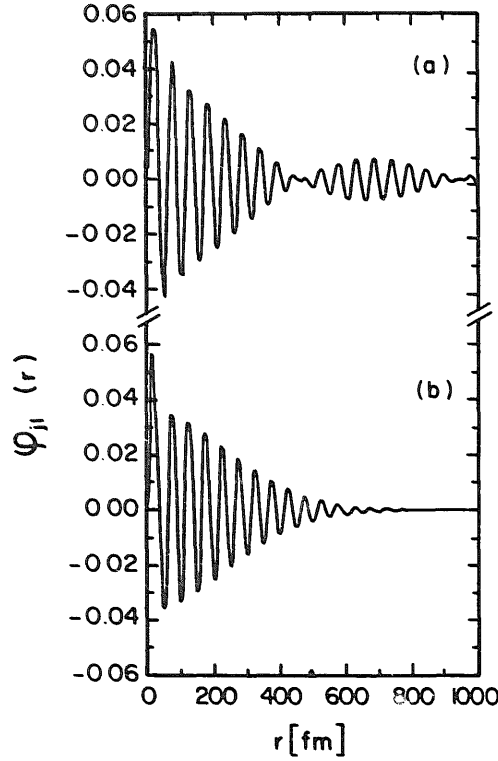


Fig. 3. Radial wavefunctions for the discretized continuum using the histogram set (a) and the continuous set (b). We used $E_j = 200$ keV, and $l = 1$.

numerical evaluation of $\langle \phi_{jlm} | r Y_{1\mu} | \phi_{j'l'm'} \rangle$ is more involved than with the second set of Γ_j functions, eq. (3.8). Indeed, as we see from fig. 3b the beats disappear with the use of the basis set (3.8). Although the use of plane-wave basis allows the derivation of simple results with both sets, this fact is of relevance for future improvement of the calculations.

Using (3.1) and the properties of the spherical harmonics one finds

$$\begin{aligned}
 V_{jlm;j'l'm'} &= \frac{(-1)^m}{\sqrt{2}} \gamma Z_T e^2 \left(Z_c \frac{m_b}{m_a} - Z_b \frac{m_c}{m_a} \right) \frac{\sqrt{(2l+1)(2l'+1)}}{(b^2 + \gamma^2 v^2 t^2)^{3/2}} \begin{pmatrix} l & 1 & l' \\ 0 & 0 & 0 \end{pmatrix} \\
 &\times \left\{ ib \left[\begin{pmatrix} l & 1 & l' \\ -m & 1 & m' \end{pmatrix} + \begin{pmatrix} l & 1 & l' \\ -m & -1 & m' \end{pmatrix} \right] + \sqrt{2} \gamma v t \begin{pmatrix} l & 1 & l' \\ -m & 0 & m' \end{pmatrix} \right\} I_{jl;j'l'},
 \end{aligned} \tag{3.9a}$$

where

$$I_{jl;j'l'} = \int r^3 dr \int dE \Gamma_j(E) \int dE' \Gamma_{j'}(E') u_{l,E}^*(r) u_{l',E'}(r). \tag{3.9b}$$

From (3.9a) one deduces that the interaction potential is different from zero only if $|l - l'| = 1$, as expected. A discussion of the use of the dipole approximation is presented in the next section.

The use of the plane-wave basis is especially useful because, exploiting the recursion and closure relations of the spherical Bessel functions, one obtains the general result

$$I_{j,l;j'l'} = \frac{\hbar^2}{\mu} \left\{ \frac{l+l'+2}{2} F_{jj'} + \delta_{l,l'+1} G_{j,j'} + \delta_{l+1,l'} G_{j',j} \right\}, \quad (3.10)$$

where

$$F_{jj'} = \int dq \Gamma_j(E) \Gamma_{j'}(E), \quad G_{jj'} = \int dq q \Gamma_j(E) \frac{d}{dq} \Gamma_{j'}(E), \quad (3.11)$$

with $E = \hbar^2 q^2 / 2\mu$. Explicit forms can be found for each basis set:

(a) Histogram. Applying this relation to the histogram set (3.6), one can show that for $j, j' \neq 0$

$$I_{j,l;j'l'} = \hbar \sqrt{\frac{2}{\mu\sigma}} \begin{cases} \frac{1}{2}(l+l'+1)[\sqrt{j} - \sqrt{j-1}] & \text{if } j = j' \\ -(-1)^{(j+l-j'-l')/2} \sqrt{\frac{1}{2}(j+j'-1)} & \text{if } |j-j'| = 1 \\ 0 & \text{otherwise.} \end{cases} \quad (3.12)$$

For $j = 0$ or $j' = 0$, only the integral with l , or $l' = 1$ is necessary, and the result is

$$I_{00;j1} = I_{j1;00} = \frac{\sqrt{2\eta\sigma}}{\pi} \frac{E_j^{3/4}}{(E_0 + E_j)^2} \left(\frac{\hbar^2}{2\mu} \right)^{3/4}, \quad (3.13)$$

where $E_j = (j - 1/2)\sigma$.

(b) Continuous basis. For the set of continuous energy functions (3.8) one finds, for $j, j' \neq 0$

$$\begin{aligned} \begin{Bmatrix} F_{jj'} \\ G_{jj'} \end{Bmatrix} &= \sqrt{\frac{\mu\sigma}{2\hbar^2}} \sum_{n,n'} C_{jn} C_{j'n'} N_n N_{n'} \\ &\times \frac{\Gamma(n^2 + n'^2 + \frac{1}{2})}{(n+n')^{n^2+n'^2+1/2}} \begin{Bmatrix} 1 \\ 2n'^2 - \frac{n'(2n^2 + 2n'^2 + 1)}{n+n'} \end{Bmatrix}, \end{aligned} \quad (3.14)$$

where $\Gamma(z)$ is the gamma function and we simplified the notation using $n \equiv n_j$. For $j = 0$, or $j' = 0$, one finds

$$I_{00;j1} = I_{j1;00} = \frac{\sqrt{2\eta\sigma}}{\pi} \frac{E_j^{3/4}}{(E_0 + E_j)^2} \left(\frac{\hbar^2}{2\mu} \right)^{3/4} \sum_n \frac{n^2!}{n^{n^2+1}} \sqrt{\frac{(2n)^{2n^2+1}}{(2n^2)!}} C_{jn}. \quad (3.15)$$

In the next section we will make use of eqs. (3.9)–(3.15) to solve numerically the coupled-channels eqs. (3.5). As we have seen above, the use of the plane-wave basis (3.3) results in the elegant derivation of $I_{j,l;j'l'}$ presented by eqs. (3.10) and (3.11). Nonetheless, the s-wave ($l = 0$) state of eq. (3.3) is not orthogonal to the bound-state wave function. To restore orthogonality one has to add an extra piece to this function. We expect however that this approximation does not affect our results appreciably since to access this state one needs at least two transitions: the $0 \rightarrow j1$ followed by the $j'1 \rightarrow j'0$. But the later transition competes with the transition to the ground state,

$j1 \rightarrow 00$, which is the dominant one. A more severe restriction is the use of plane waves to describe the continuum. A realistic calculation would have to use outgoing waves for $u_{l,E}^{(+)}(r)$ which would carry information about the final-state interactions of the (b+c) system.

4. Results and discussions

In this section we use the theory delineated in the last section to study the break-up of ^{11}Li projectiles incident on heavy targets at energies around 100 MeV/nucleon. In fig. 4 we show the integrals I_{j_l,j'_l} for the continuum-continuum coupling ($j, j' \neq 0$). In particular we choose $l = 0$ and $l' = 1$. The coupling $j0 \rightarrow j' = j, 1$, shown in fig. 4a (solid line), is a reorientation effect in which the transition involves only a change in the angular momentum ($l = 0$ to $l = 1$ in this case) of the state. In the fig. 4a (dashed line) we plot I_{j_0,j'_1} for a transition between states with different energies. In particular we take the transition between neighboring states, with $j' = j + 1$. We use the results obtained with the continuous energy set, eqs. (3.14) and (3.15). One observes that while the integral for the jj coupling decreases with energy, the one for the $j, j + 1$ coupling increases steadily. These results reproduce the trend shown by eq. (3.12). In fig. 4b it is shown how I_{j_0,j'_1} varies as a function of E'_j , for a fixed $E_j = 0.2$ MeV. One observes that it is maximum for neighbouring energy states and has an oscillatory behaviour. This has as a consequence that the $j, j' \neq j$ coupling will practically not contribute to the total break-up probability, $P_{(E)}^{\text{BU}}$, since its contribution will be washed out.

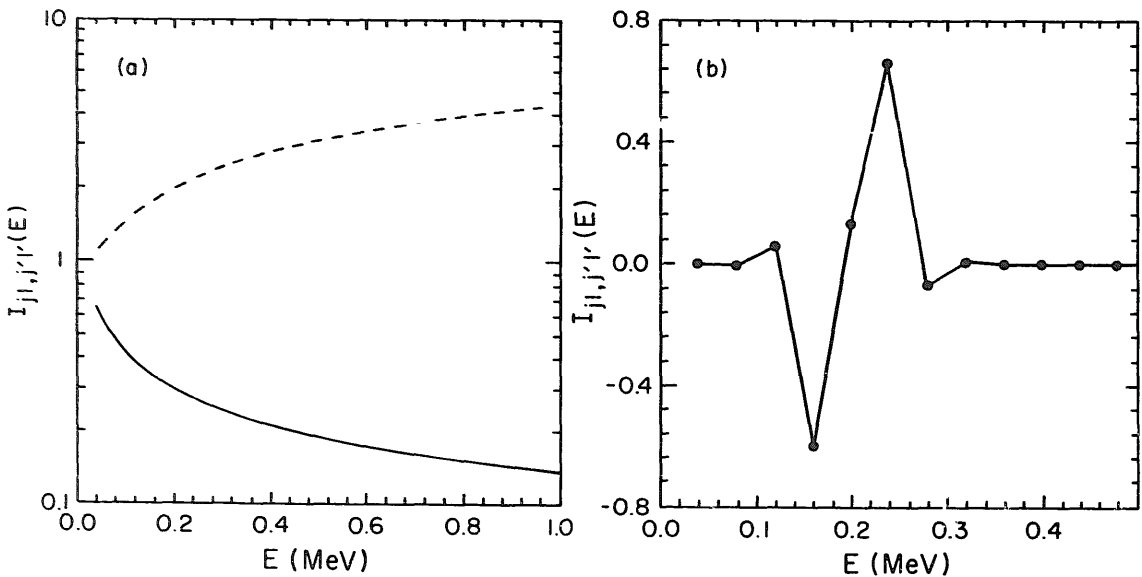


Fig. 4. (a) Radial matrix elements, eq. (3.9b), for the transition $j \rightarrow j + 1$ (dashed line), and for the $j \rightarrow j$ one (solid line). We used $l = 0$ and $l' = 1$. (b) Radial matrix elements for the transition $j \rightarrow j'$, keeping $E_j = 200$ keV and varying E'_j .

The break-up probability per unit energy interval, $P_{(E)}^{\text{BU}}$, is given by

$$P_{(E)}^{\text{BU}} = \sum_{ij} \Gamma_i(E) \Gamma_j(E) Q_{ij}, \quad (4.1a)$$

where

$$Q_{ij} = \text{Re} \left[\sum_{lm} a_{ilm}^* a_{jlm} \right]. \quad (4.1b)$$

In fig. 5 we show the break-up probability per unit energy interval for the reaction $^{11}\text{Li} + \text{Pb}$ at 100 MeV/nucleon and $b = 15\text{fm}$, calculated from eq. (4.1) by solving the coupled differential equations (3.5) for a_{ilm} . We see that the energy distribution of the fragments is peaked at $E \sim 0.2\text{ MeV}$. Therefore, the most relevant momentum transfer to the ^{11}Li nucleus occurs at $q = \sqrt{2\mu_{bc}E}/\hbar \sim 20\text{fm}^{-1}$. The validity of the dipole approximation for the interaction potential (3.9) to calculate the continuum-continuum coupling can only be justified for $qr \ll 1$. But, as shown in fig. 3, the discretized wavefunctions extend up to 400 fm. Thus, unless the matrix elements for the continuum-continuum coupling, eq. (3.9b), have its main contribution from $r \ll 20\text{ fm}$, the dipole approximation is not valid. The j_j coupling do satisfy this requirement. In this case the wavefunctions have equal energies, but different angular momenta. This causes an asymptotically ($r \gg 1/q$) constant phase difference between the wavefunctions entering in $I_{j_l, j_l'}$. This leads to cancellations in the integrand of eq. (3.9b) for large r . The situation is different for the $(j, j' \neq j)$ coupling. In this case the integrand has contributions from larger values of r and these contributions increase with the energy. With a correct treatment of the multipole expansion of the interaction potential (2.1) the integrals $I_{j_l, j_l' \neq j_l}$ would decrease with E . We expect

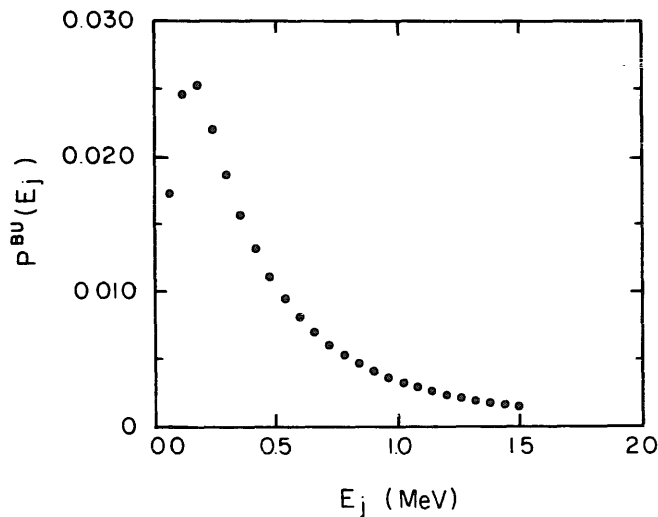


Fig. 5. Coulomb break-up probability, per unit energy interval (MeV^{-1}), of ^{11}Li projectiles incident on lead at 100 MeV/nucleon and $b = 15\text{ fm}$, as a function of the final total kinetic energy of the fragments.

that the transitions between $00 \rightarrow j', l = 1$ and $j', l = 1 \rightarrow 00$ dominate the excitation process, so that the matrix elements between states with $j \neq j' \neq 0$ do not play an important role. Also, to minimize the consequence of the breaking down the dipole approximation in the continuum-continuum coupling at $j \neq j'$, we use in our calculation a large parameter K (we take $K = 4$). This leads to small $I_{j \neq j'}$.

In fig. 6 the solid line represents P^{BU} , the total break-up probability [eq. (4.1) integrated over energy], as a function of the adimensional parameter $\tau = vt/b$, for $b = 15$ fm. This is obtained by solving the coupled-channels equations (3.5) for a time t and calculating the sum $P^{\text{BU}}(t) = \sum_{jlm} |a_{jlm}|^2$. The dashed line corresponds to the neglect of all transitions, except for the $0 \rightarrow jl$ ones. In the low-energy limit, eq. (2.6), this gives the same result as eq. (2.7). The solid line includes all possible transitions. The break-up probability occurs in a time scale of $\Delta t \sim b/v$. As $t \rightarrow \infty$ the break-up probability is 40% smaller than that calculated by first-order perturbation theory.

The total cross section is given by

$$\sigma^{\text{BU}} = 2\pi \int_{b_{\text{min}}}^{\infty} b db P^{\text{BU}}(\infty). \quad (4.2)$$

The value of b_{min} is chosen, according to Winther and Alder⁶), as

$$b_{\text{min}} = R_{\text{P}} + R_{\text{T}} + \frac{\pi Z_{\text{P}} Z_{\text{T}} e^2}{4E_{\text{lab}}}, \quad (4.3)$$

where $R_{\text{P}}(R_{\text{T}})$ is the projectile (target) radius. For ^{11}Li we use $R_{\text{P}} = 3.14$ fm, while for the target we use $R_{\text{T}} = 1.2A^{1/3}$ fm. The above formula includes a recoil correction on the Coulomb excitation cross section, given by the last term which depends on the bombarding energy⁶), E_{lab} . Our results are shown in table 1. In the second column we give the cross sections within our non-perturbative approach, while in the first column we give the prediction of first-order perturbation. The experimental values for the

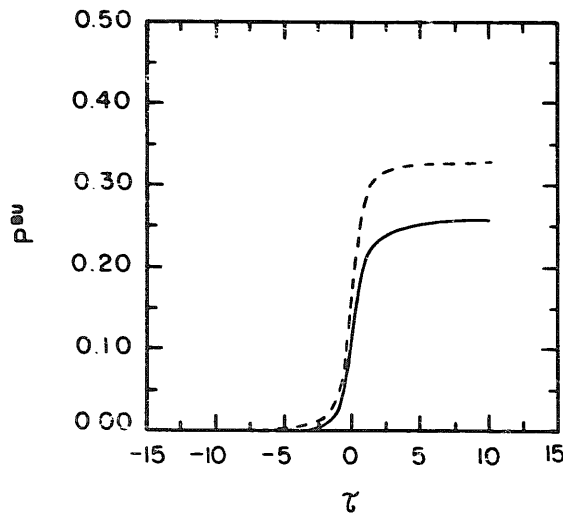


Fig. 6. Coulomb break-up probabilities of ^{11}Li projectiles incident on lead at 100 MeV per nucleon, as a function of $\tau = b/v$.

TABLE I

Comparison among the cross sections for the Coulomb break-up of ^{11}Li incident on lead, obtained within the first-order perturbation, $\sigma^{(1)}$, and with the coupled-channels calculation, σ . The last column gives the experimental values of refs. ^{2,7}).

E_{lab} [MeV/nucleon]	$\sigma^{(1)}$ [b]	σ [b]	σ_{exp} [b]
790	1.01	0.94	0.89 ± 0.1
86.2	3.5	2.8	1.37 ± 1.43
69.9	3.8	3.1	2.96 ± 0.83

electromagnetic dissociation cross section of ^{11}Li projectiles incident on Pb at several bombarding energies are shown in the third column ^{2,7}). It is not clear from the experimental data of ref. ²) which fraction of these cross sections go into the $^9\text{Li} + 2n$ channel, but due to its binding energy the break-up probability into this channel is dominant and a direct comparison with our results is possible. We see that, while for high bombarding energies the results of the two theoretical approaches are practically the same, at low energies they differ by about 20%. This is due to the large break-up probabilities which occur for reactions around some tens of MeV per nucleon ⁸). The coupled-channels calculation result gives a better value of the cross section at this energy.

5. Conclusions

We have developed a non-perturbative coupled-channels calculation for the break-up of weakly bound nuclei. Since we wanted to access the qualitative aspects of a non-perturbative approach to the break-up, the simple cluster model was used for the purpose. We studied the particular case of the Coulomb break-up of ^{11}Li projectiles. The general features of our results should also apply to the break-up of other weakly bound nuclei. The continuum was discretized in order to obtain non-divergent matrix elements for the continuum-continuum coupling. Our calculations were not intended to give an accurate description of the break-up process, but to serve as a support for more fundamental ones, where a more realistic treatment of the ground and final state of the projectile is accomplished as, e.g., that of ref. ⁹). Our main conclusion is that a non-perturbative treatment of the Coulomb break-up of loosely bound nuclei as, e.g., ^{11}Li is needed at low-energy collisions (10-100 MeV/nucleon). The non-perturbative cross section gives a total cross section 20% lower than the predictions of first-order perturbation theory.

We also have found that the continuum-continuum coupling can be fairly well treated by means of a discretization with help of strongly peaked functions. In order

to avoid spurious oscillations in the discretized wavefunctions which can lead to slowly convergent integrals for the matrix elements, a set of continuous functions was introduced for the discretization procedure. The final relative motion energy of the fragments is found to be very small, of order of their binding energy. Thus, it is expected that the interactions between the fragments distort their final states appreciably. The continuum-continuum coupling may therefore be much more relevant than what we obtained with our calculations. The results presented in this article will certainly help to understand these and other related questions in the future.

We have benefited from very useful discussions with Prof. R. Donangelo.

This work was supported in part by the CNPq-Conselho Nacional de Desenvolvimento Científico e Tecnológico/Brazil and the NSF-National Science Foundation/USA, under grant PHY-9017077

References

- 1) I. Tanihata, Nucl. Phys. **A522** (1991) 275c
- 2) B. Blank *et al.*, Z. Phys. **A340** (1991) 41
- 3) C.A. Bertulani and G. Baur, Nucl. Phys. **A480** (1988) 615;
C.A. Bertulani and M.S. Hussein Phys. Rev. Lett. **64** (1990) 1099;
C.A. Bertulani, G. Baur and M.S. Hussein, Nucl. Phys. **A526** (1991) 751
- 4) H.J. Bär and G. Soff, Physica **C128** (1985) 225
- 5) F.W. Byron and R.W. Fuller, Mathematics of classical and quantum physics, vol. 1 (Addison-Wesley, New York, 1969) p. 148
- 6) A. Winther and K. Alder, Nucl. Phys. **A319** (1979) 518
- 7) T. Kobayashi *et al.*, Phys. Lett. **B232** (1989) 51
- 8) M.S. Hussein, M. Pato and C.A. Bertulani, Phys. Rev. **C44** (1991) 2219
- 9) G.F. Bertsch and H. Esbensen, Ann. of Phys. **209** (1991) 327;
H. Esbensen and G.F. Bertsch, Nucl. Phys. A, submitted